Lubricant film flow and depletion characteristics at head/disk storage interface*

Hong-Rui Ao(敖宏瑞)[1,†], Zhi-Ying Han(韩志英)[1], Kai Zhang(张凯)[1], and Hong-Yuan Jiang(姜洪源)[1]

School of Mechatronics Engineering, Harbin Institute of Technology, Harbin 150001 *China*

(Received 5 May 2016; revised manuscript received 4 August 2016; published online 25 October 2016)

The characteristics of lubricant film at head/disk interface (HDI) are essential to the stability of hard disk drives. In this study, the theoretical models of the lubricant flow and depletion are deduced based on Navier–Stokes (NS) and continuity equations. The air bearing pressure on the surface of the lubrication film is solved by the modified Reynolds equation based on Fukui and Kaneko (FK) model. Then the lubricant film deformations for a plane slider and double-track slider are obtained. The equation of lubricant film thickness is deduced with the consideration of van der Waals force, the air bearing pressure, the surface tension, and the external stresses. The lubricant depletion under heat source is simulated and the effects of different working conditions including initial thickness, flying height and the speed of the disk on lubricant depletion are discussed. The main factors that cause the lubricant flow and depletion are analyzed and the ways to reduce the film thickness deformation are proposed. The simulation results indicate that the shearing stress is the most important factor that causes the thickness deformation and other terms listed in the equation have little influence. The thickness deformation is dependent on the working parameter, and the thermal condition evaporation is the most important factor.

Keywords: lubricant film, depletion, deformation characteristics, head/disk interface

PACS: 46.55.+d, 47.15.gm, 68.03.–g **DOI:** 10.1088/1674-1056/25/12/124601

1. Introduction

Reducing the flying height of a slider is an effective way to improve the storage capacity of a hard disk. As the flying height is close to 3.5 nm which is comparable to the thickness of lubricant film lubed on the disk surface, the areal density reaches 1 Tb/in^2 (1 in = 2.54 cm). Under this condition, the characteristics of the lubricant film at head/disk interface (HDI) and its operational performance influence the dynamic features of the slider.

It is necessary to choose the magnetic medium material with high coercivity to improve the areal storage density of the disk, but the high coercivity makes it difficult to write information onto the disk. Figure 1 shows the working principle of the heat-assisted magnetic recording (HAMR) technology. The laser beam increases the temperature of the magnetic medium sharply, and then writes the information quickly so the temperature will decrease to normal. In this way the high coercivity can protect the information.[1] In this process, the lubricant on the disk suffers high temperature which reaches several hundred degrees, and the evaporation will occur on the lubricant film according to the working condition.[2]

There have been many studies on the characteristics of lubricant film. In the experimental study of Watanabe and Bogy, the flight attitude was related to the surface topography of the slider, and the flow of lubricant and recovery of lubricant film thickness were observed when the head moved; in some conditions the lubricant even moved from disk surface to the head.[3] By molecular dynamic simulations, static and dynamic characteristics of lubricant were studied based on a coarse-grained bead-spring model which was adopted to investigate the molecular conformation, bead density, end bead density and the dynamic properties.[4,5] In the model of Jing *et al.*, the typical thin-film lubrication mechanism was analyzed by using the interfacial disjoining pressure to characterize the dominant role in the solid–lubricant interaction on a microscale, and then the lubrication Stribeck curve based on thermodynamic concepts was established.[6] Moreover, the lubricant loss and its influencing factors were examined in the studies. In the model of Ma and Liu the lubricant film loss in a short time and sedimentation process on the disk were studied experimentally based on the principle of evaporation and deposition.[7] In another work, a simplified second-order model based on the Poiseuille flow was put forward to simulate the dynamic behavior of ultra-thin gas film at HDI.[8] The surface tension relating to temperature and film thickness, as well as the factors influencing the lubricant transfer, such as the sedimentary processes of hydrone, the hydrosoluble electrolyte and alkali halide, was considered in the calculation of lubricant film thickness deformation.[9,10] The effect of shear extrusion on rarefied gas lubrication performance influence was investigated under the mode of roughness.[11] It can be seen from these studies that the lubricant flow is a complex problem, and it is difficult to obtain an overall method or expressions to describe its flow characteristics.

*Project supported by the National Natural Science Foundation of China (Grant No. 51275124).

†Corresponding author. E-mail: hongrui_ao@hit.edu.cn

© 2016 Chinese Physical Society and IOP Publishing Ltd

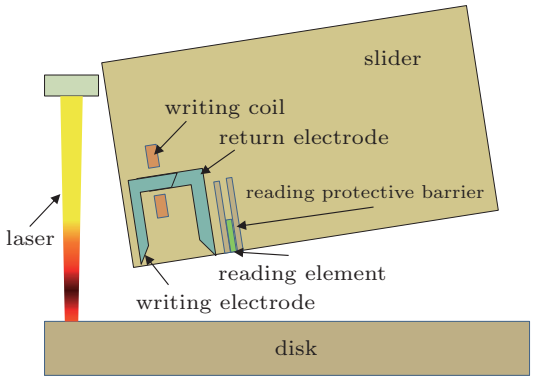


Fig. 1. (color online) Interface of the HAMR slider system.

According to the previous study, when the flying height is much larger than the lubricant film thickness, the effects of the lubricant film on the dynamic characteristics at HDI can be ignored completely. But when the flying height decreases continuously and approaches to the same level as the lubricant film thickness, the dynamic characteristics of the head will change since the air bearing stress causes both the distribution and flow status of lubricant film to change. In this study, the classical FK model is used to modify the Reynolds' equation by considering the Poiseuille flow rate.[12] As a result, it is necessary to study the flow, loss and recovery of lubricant film and relevant influencing factors under operational condition. It is noted that in order to maintain the best tribological performance and stability of the slider at HDI, the lubricant film thickness on the disk surface must be uniformly distributed. In this study, the deformations of lubricant film under different flying heights and heat sources are theoretically described in a synthesized way, and the main influencing factors and working parameters relating to the dynamic behavior and tribological performance at HDI are discussed. The results will be beneficial to the design of the air bearing slider at head/disk interface.

2. Theoretical model of film thickness deformation

In this section the equation of lubricant film thickness deformation is deduced with the consideration of the lubricant flow and the influence of heat sources.

2.1. Modified Reynolds' equation and air bearing stress

A schematic diagram of the head/disk interface is shown in Fig. 2, in which $\alpha(t)$ is the pitch angle of the slider as a function of time, h_{G0} is the flying height, and U_0 is the velocity.

The read/write element is embedded in a slider which flies over the disk. When the disk rotates at a high speed, the air dynamic pressure is formed in the gap, and the balanced cantilever puts a pre-loading on the slider so that the head can keep a stable flying height at a few nanometers height above the disk. In order to describe the dynamic pressure characteristics of the compressible gas and calculate the air bearing stress at head/disk interface, some assumptions are given as follows.

(i) The gas is in ideal condition;

(ii) The flow of the gas is laminar and thermostatical;

(iii) The gas is Newtonian fluid;

(iv) The body stress is ignored;

(v) The thickness of gas film is much smaller than the slider's spatial size.

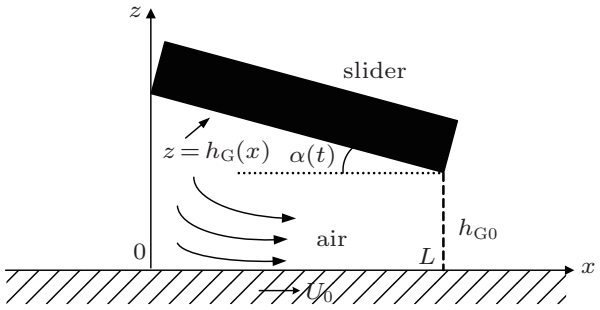


Fig. 2. Sketch map of air bearing.

The modified Reynolds' equation can be derived by considering the rarefaction effect of ultra-thin air film, and expressed as follows:

$$\begin{aligned}&\frac{\partial}{\partial x}\left(p_G h_G^3 Q\frac{\partial p_G}{\partial x}\right)+\frac{\partial}{\partial y}\left(p_G h_G^3 Q\frac{\partial p_G}{\partial y}\right)\\ &=6U\mu_G\frac{\partial}{\partial x}(p_G h_G)+6V\mu_G\frac{\partial}{\partial y}(p_G h_G)\\ &\quad+12\mu_G\frac{\partial}{\partial t}(p_G h_G),\end{aligned}\tag{1}$$

where U and V are the relative velocity of gas flow at the head/disk interface in the x and y direction (in units m/s), respectively. The correction factor Q is based on the FK model,[12] $Q = Q_p/Q_{con}$, where Q_p and Q_{con} are the discharge coefficients of Poiseuille flow and continuous Poiseuille flow, respectively; p_G is the gas pressure (in unit Pa), μ_G is the gas viscosity (in units Pa·s), h_G is the distance of the slider and disk (in unit m), and t is the time (in unit s).

2.2. Film thickness deformation equation

When the gap between the head and disk is comparable to the thickness of lubricant film, the interaction of the air motion and the lubricant film will be crucial. The lubricant film interface will not be considered as plane any more since its flow is caused by the air bearing stress and the intermolecular stress. The air bearing stress will consequently change with the flow of the lubricant film.

Figure 3 shows the stresses on lubricant interface, in which h_0 is the initial film thickness, τ is the external tangential stress, Π is the external normal stress, and ϕ is the volume stress. In this study, the lubricant is PFPE-Z.

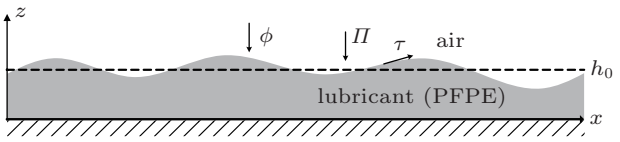


Fig. 3. Stress of lubrication film.

The lubricating film flow model is established based on the Navier–Stokes (NS) equations and continuity theory of the flow. The NS equations and the continuity equation are shown as follows:

$$\begin{cases} \rho\left(\dfrac{\partial u}{\partial t}+u\dfrac{\partial u}{\partial x}+w\dfrac{\partial u}{\partial z}\right)=-\dfrac{\partial p}{\partial x}+\mu\nabla^2 u-\dfrac{\partial \phi}{\partial x}, \\ \rho\left(\dfrac{\partial w}{\partial t}+u\dfrac{\partial w}{\partial x}+w\dfrac{\partial w}{\partial z}\right)=-\dfrac{\partial p}{\partial z}+\mu\nabla^2 w-\dfrac{\partial \phi}{\partial z}, \\ \dfrac{\partial u}{\partial x}+\dfrac{\partial w}{\partial z}=0, \end{cases} \tag{2}$$

where ρ is the lubricant density (in units kg/m^3), μ is the lubricant viscosity (in units Pa·s), p is the external stress at the interface (in unit Pa), ∇^2 is the Laplace operator, u and w are the velocities of lubricant film in the x and z directions (in units m/s), respectively.

The boundary conditions of the lubricant film are defined as follows.

For $z=0$,

$$\begin{cases} w=0, \\ u=0. \end{cases} \tag{3}$$

For $z=h(x,t)$,

$$\begin{cases} w=\dfrac{\partial h}{\partial t}+u\dfrac{\partial h}{\partial x}, \\ \Lambda\cdot\boldsymbol{n}=-\kappa\sigma\boldsymbol{n}+\dfrac{\partial \sigma}{\partial s}\boldsymbol{t}+p, \end{cases} \tag{4}$$

where Λ is the lubricant stress tensor (in unit Pa), $\boldsymbol{n}$ is the unit vector of vertical interface, $\boldsymbol{t}$ is the unit tangent vector, h is the lubricant film thickness (in unit m), κ is the average curvature of interface (in unit m^{-1}), s is the arc length along the interface (in unit m), and σ is the surface tension coefficient.

The first formula in Eq. (4) is used to balance the normal velocity of the boundary. The second one includes two parts: one is the equilibrium relationship between the external tangential stress, τ, and the gradient of surface tension coefficient, σ; the other one is the equilibrium relationship between the stress tensor which is subtracted from the normal part of external stress and the average curvature of surface tension. The stresses on the boundary are tangential stress, normal external stress, surface tension and conservative body stress.

The mass conservation equation can be obtained by integrating the continuity equation with the boundary equations, shown as

$$\frac{1}{u_0}\frac{\partial h}{\partial t}+h_0\frac{\partial}{\partial x}\left(\int_0^h u\,\mathrm{d}z\right)=0, \tag{5}$$

where u_0 is the initial velocity of lubricant film in the x direction (in units m/s), and h_0 is the initial film thickness (in unit m).

Transform and integrate the NS equations, and then substitute its resulting equation into the mass conservation equation (5) to obtain the equation of lubricant film thickness as follows;

$$\mu\frac{\partial h}{\partial t}+\nabla\left[\frac{1}{2}h^2(\tau+\nabla\sigma)\right] -\nabla\left[\frac{1}{3}h^3\nabla(\phi-\sigma\nabla^2 h-\Pi)\right]=0, \tag{6}$$

where ∇ is Hamiltonian operator.

For a hard disk drive in operational state, the normal stress on the lubricant film includes the external stress Π which is the integral of the air bearing p_{G}, the normal part of surface tension $\sigma\nabla^2 h$ (Laplace stress), and the volume stress ϕ. The shearing stress is comprised of the stress in tangential direction caused by air bearing stress τ and the gradient of surface tension coefficient σ which is constant at normal temperature. The volume stress is calculated as follows:

$$\phi=A_{\mathrm{d}}/6\pi(h+d_0)^3, \tag{7}$$

where A_d is the Hamaker constant (in units N·m), and d_0 is the acting radius of van der Waals force (in unit m).

The external tangential stress caused by air bearing force is expressed as follows:

$$\begin{cases} \tau_x=\dfrac{h_{\mathrm{G}}}{2}\dfrac{\partial p_{\mathrm{G}}}{\partial x}-\dfrac{\mu_{\mathrm{G}}u}{2a\lambda+h_{\mathrm{G}}}, \\ \tau_y=\dfrac{h_{\mathrm{G}}}{2}\dfrac{\partial p_{\mathrm{G}}}{\partial y}-\dfrac{\mu_{\mathrm{G}}v}{2a\lambda+h_{\mathrm{G}}}, \end{cases} \tag{8}$$

where λ is the mean free path of air molecules (in unit m), a is a constant coefficient, u and v are the velocity of lubricant film in the x and y direction (in units m/s), τ_x and τ_y are the external tangential stress in the x and y direction, respectively.

The shearing stress is the linear combination of the Poiseuille flow and the Couette flow which are related to the gradient of air bearing stress. It can be seen from Eq. (7) that the lubricant thickness deformation is caused by the combined actions of the air bearing stress, surface tension and van der Waals force.

2.3. Deformation of lubricant film under the heat source

The local transient temperature on the disk surface under heat source may reach to hundreds of Celsius degrees when the heat-assisted magnetic recording (HAMR) technology is applied. The stress diagram of lubricant in HAMR is shown in Fig. 4, and the lubricant film has a constant thickness for simplification.

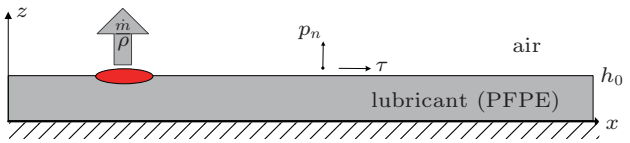


Fig. 4. (color online) Stresses of lubrication film with heat source.

If the surface temperature is higher than the saturation temperature, the lubricant will evaporate strongly. The lubricant thickness deformation with the consideration of evaporation is expressed as

$$\frac{\partial h}{\partial t}+\nabla\left[\frac{1}{2\mu}h^2(\tau+\nabla\sigma)\right]-\nabla\left[\frac{1}{3\mu}h^3\nabla p_{\rm n}\right]+\frac{\dot{m}}{\rho}=0, \quad (9)$$

where p_n is the normal stress on the lubricant surface (in unit Pa), and $\dot{m}$ is the volume flow rate caused by evaporation (in units kg/(m^2·s)).

The lubricant viscosity decreases with the increase of temperature if the temperature rises considerably. Moreover, the lubricant thickness is so small that the relationship between viscosity and thickness cannot be ignored. The viscosity of fluid film is expressed as[10]

$$\mu=\left(\frac{N_{\rm A}h_{\rm p}}{V_l}\right)\exp\left(\frac{\Delta E_{\rm vis}-T\Delta S_{\rm vis}}{RT}\right). \quad (10)$$

where $N_{\rm A}$ is the Avogadro constant (in unit /mol), $h_{\rm p}$ is the Planck constant (in units J·s), V_l is molar volume of lubricant (in units m^3/mol), R is the gas constant (in units J/(mol·K)), T is the system temperature (in unit K), $\Delta E_{\rm vis}$ is the activation energy (in units J/mol), and $\Delta S_{\rm vis}$ is the flowing enthalpy (in units J/mol). In addition, $\Delta E_{\rm vis}$ and $\Delta S_{\rm vis}$ are related to liquid thickness.

The dependences of viscosity on lubricant thickness and temperature are shown in Fig. 5. The viscosity decreases sharply when the thickness reaches a critical value. In addition, the critical thickness becomes smaller when the temperature increases. Therefore, it can be predicted that the lubricant thickness has a limit.

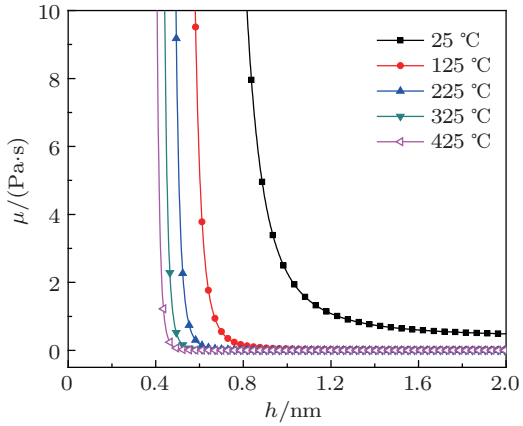


Fig. 5. (color online) Dependences of lubricant viscosity on lubricant film thickness and temperature.

When the heat source is considered, the temperature gradients in the fluid will lead to different surface tensions, and produce a shearing stress (thermal-capillary stress):

$$\tau_{\rm tc}=\frac{{\rm d}\sigma}{{\rm d}T}\frac{\partial T}{\partial x}\boldsymbol{e}_1+\frac{{\rm d}\sigma}{{\rm d}T}\frac{\partial T}{\partial y}\boldsymbol{e}_2, \quad (11)$$

where $\boldsymbol{e}_1$ and $\boldsymbol{e}_2$ are the unit vectors in x and y directions, respectively.

In the HAMR system, the effect of air bearing force is ignored. The pressure of lubricant film surface, p, consists of disjoining stress, ϕ, and Laplace stress, $\sigma\nabla h^2$. The expression of the lubricant thickness is

$$\frac{\partial h}{\partial t}+\frac{\partial}{\partial x}\left[-\frac{1}{\mu}\frac{A_{\rm d}}{h}\frac{\partial h}{\partial x}+\frac{\sigma}{3\mu}h^3\left(\frac{\partial^3 h}{\partial x^3}+\frac{\partial^3 h}{\partial x\partial y^2}\right)-\frac{\gamma}{2\mu}\frac{\partial T}{\partial x}h^2\right]+\frac{\partial}{\partial y}\left[-\frac{1}{\mu}\frac{A_{\rm d}}{h}\frac{\partial h}{\partial y}+\frac{\sigma}{3\mu}h^3\left(\frac{\partial^3 h}{\partial y^3}+\frac{\partial^3 h}{\partial x^2\partial y}\right)-\frac{\gamma}{2\mu}\frac{\partial T}{\partial y}h^2\right]+\frac{\dot{m}}{\rho}=0, \quad (12)$$

where γ is the thermal conductivity coefficient of surface tension.

Evaporativity rises in proportion to the difference in value between the balance pressure of evaporation and its current pressure according to the kinetic theory, and is expressed as

$$\dot{m}=\alpha\left(\frac{M_{\rm m}}{2\pi RT}\right)^{1/2}(p_{ev}-p_v), \quad (13)$$

where M_m is the molar volume of fluid molecular (in units m^3/mol), $p_{\rm ev}$ is the balanced evaporating pressure (in unit Pa), p_v is the current evaporating pressure (in unit Pa), and α is the adjustment coefficient.

According to Eq. (13), the net evaporation will occur if the current pressure is larger than the balance pressure deduced based on the chemical potential energy of liquid and gas, and its expression is written as

$$p_{\rm ev}=p_{\rm vap}\exp\left[\frac{M_{\rm m}}{\rho RT}(-\phi-\sigma\nabla^2 h)\right], \quad (14)$$

where $p_{\rm vap}$ is the evaporating pressure of unit volume (in unit Pa) and expressed as

$$p_{\rm vap}=p_{\rm vap0}\exp\left[-\frac{\Delta H_{\rm vap}}{R}\left(\frac{1}{T}-\frac{1}{T_0}\right)\right], \quad (15)$$

with $H_{\rm vap}$ being the enthalpy of vaporization (in units J/mol), and $p_{\rm vap0}$ denoting the evaporating pressure per unit volume (in unit Pa) for a given reference temperature $T_0=35$ °C.[13]

3. Results and discussion

3.1. Finite element analysis and simulation results

In the study, a plane slider and double-track slider are adopted, and the physical dimensions are shown in Fig. 6. Other parameters are given in Table 1. The finite element method is used to simulate the characteristics of lubricant film and dynamic behavior of air bearing and sliders.

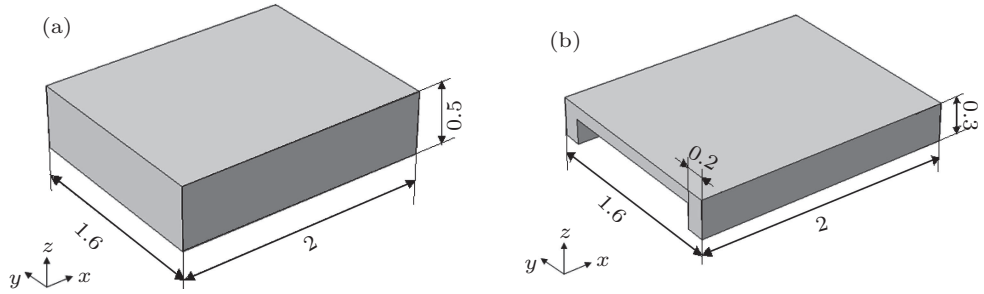


Fig. 6. Structure models of (a) plane slider and (b) double-track slider.

Table 1. Parameters of the hard disk drive.

Flying height/nm	Disk revolving speed/rpm	Pitching angle/μrad	Roll angle/μrad	Air viscosity/Pa·s	Mean free path of air molecular/nm	Ambient temperature/°C	Gas constant/[J/(mol·K)]
10	5400	150	0	1.83×10^{-5}	65	35	287.03

The air bearing stress is obtained by solving the modified Reynolds' equation (Eq. (4)). Figure 7 shows the pressure distributions on the working surfaces of the plane slider and the double-track slider, respectively. The simulation results show the pressure distribution shape of the plane slider with peak values. The stress on the surface of the slider can be calculated by integrating the pressure distribution. The stress on the plane slider is 6.864 N, which is ten times larger than that of the double track slider.

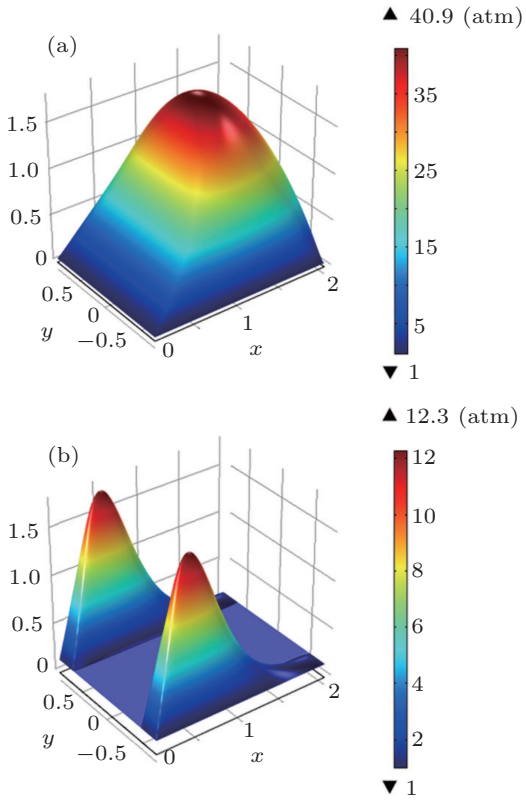


Fig. 7. (color online) Distributions of the surface pressure for (a) plane slider and (b) double-track slider. The unit 1 atom = 1.01325×10^5 Pa.

The tangential stress caused by the air bearing stress can be calculated by using Eq. (8) as shown in Fig. 8.

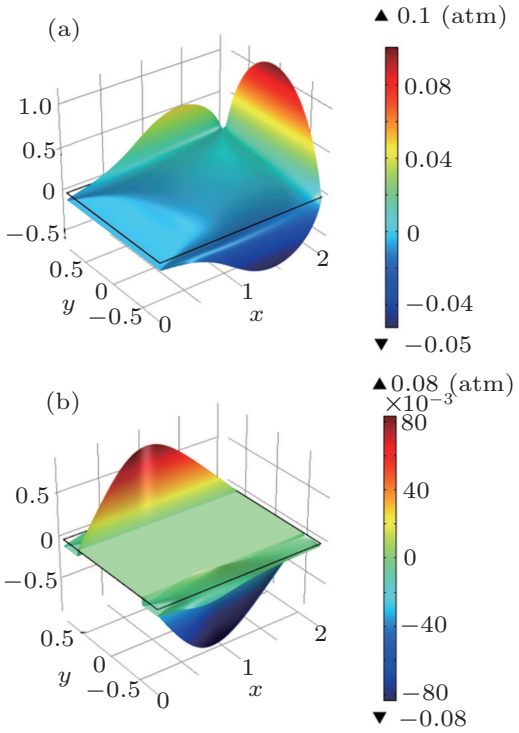


Fig. 8. (color online) Distributions of the surface tangential stress for (a) plane slider and (b) double-plane slider.

The high temperature of the lubricant influences its viscosity and thus leads to its evaporation. Consequently, under the action of heat source, the lubricant film thickness decreases at the partial position. In the present study, the lubricant thickness deformation is obtained with the consideration of the stress distribution and heat source. Figure 9 shows the thickness distribution on the disk surface after 5-min flying of sliders, where R is the range in radial direction (in unit mm) and L means the range in circumferential direction. It can be seen that the thickness deformation changes evidently in width for the plane slider, its initial thickness is 1.25 nm, and the extreme values of thickness deformation are 14.312 Å and 11.227 Å after 5 minutes. As for the double-track slider,

the thickness deformation changes evidently in the area below the tracks, and its extreme values are 13.057 Å and 11.649 Å.

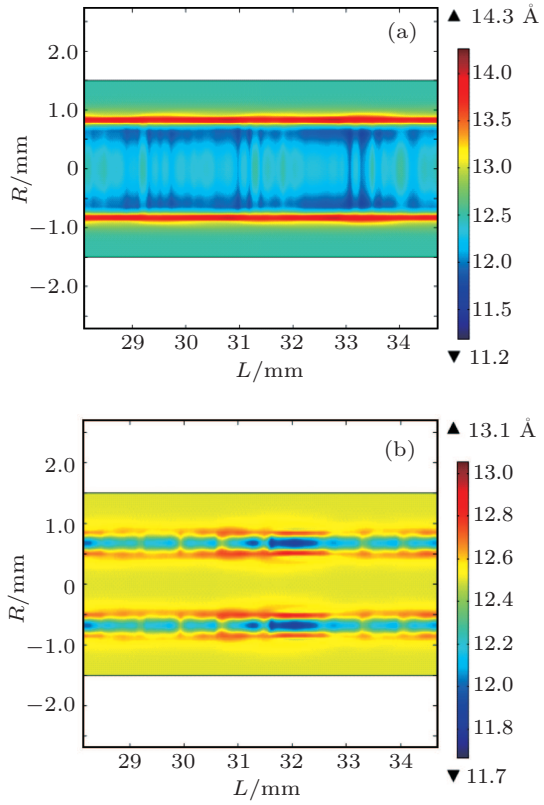


Fig. 9. (color online) Simulation results of the lubricant thickness deformation for (a) plane slider and (b) double-track slider.

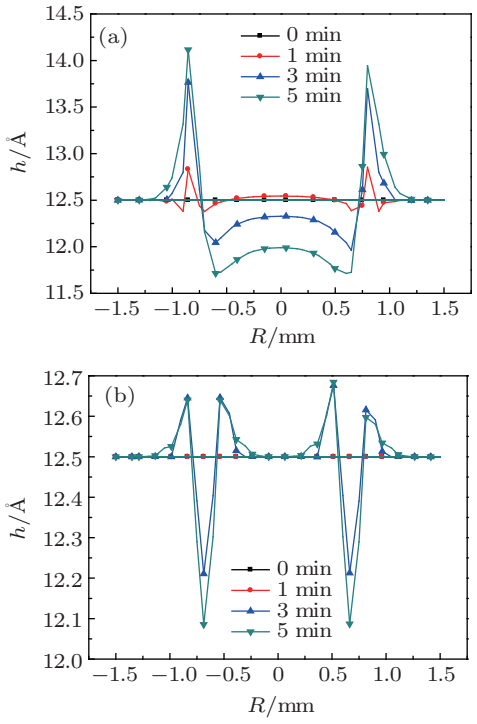


Fig. 10. (color online) Radial sections of the lubricant thickness for (a) plane slider and (b) double-track slider.

Then, the film deformation on the cross section of disk along the radial direction is analyzed. Figure 10 shows the lubricant thickness deformations at different times such as 0 min, 1 min, 3 mins, and 5 mins later. The slider flies above the disk repeatedly, and the thickness deformation changes dramatically with time. As for the plane slider there are very sharp peaks on both sides of the slider. The minimum value of the film thickness which is related to the initial thickness occurs in the center of the slider. As for the double-track slider, there are two symmetric hollow losses on the cross section of lubricant film, and their sites correspond to the positions of the tracks. The lubricant is pushed up on both sides of the track, and no changes happen in the center of the slider. Remarkable changes occur on the film deformation from 1 min to 3 min, but as time goes by, the change becomes slow. For the double-track slider, after 5 min, the peak changes from 1.8 Å to 0.872 Å, which is related to the initial film thickness. It indicates that the lubricant movement is influenced by the surface topography of the slider significantly.

3.2. Effect of physics parameters on the lubricant flow

According to Eq. (7), the physical parameters which affect the film thickness are air bearing stress, shearing stress, separating stress, and surface tension. In this study, the influence of external stress on the lubricant flow is analyzed. The air bearing stress and the shearing stress are ignored separately in the simulation. Figure 11 shows the effects of air bearing stress on the film thickness distribution. When the shearing stress is ignored, there is little fluid movement. Then, it can be concluded that the air bearing stress has little influence on the lubricant film deformation, and the shearing stress is a decisive factor.

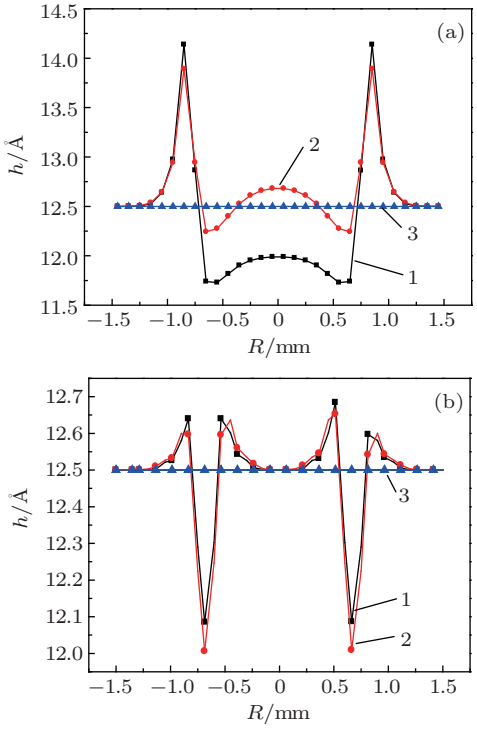


Fig. 11. (color online) Effects of external normal and tangential stress for (a) plane slider and (b) double-track plane (1: all stresses, 2: no pressure, 3: no shearing stress).

According to Eq. (9), the shearing stress is combined by Poiseuille flow term and Walcott flow term. Figure 12 shows the influences of Poiseuille flow and the Walcott flow on lubricant thickness deformation. The Walcott flow causes the extreme value to be larger, especially on the double-track slider. Therefore, this item should be kept in the equation for the accuracy of the simulation results. The shearing stress can be reduced effectively by reducing the gradient of air bearing stress because the Poiseuille flow is related to the gradient of air bearing stress primarily.

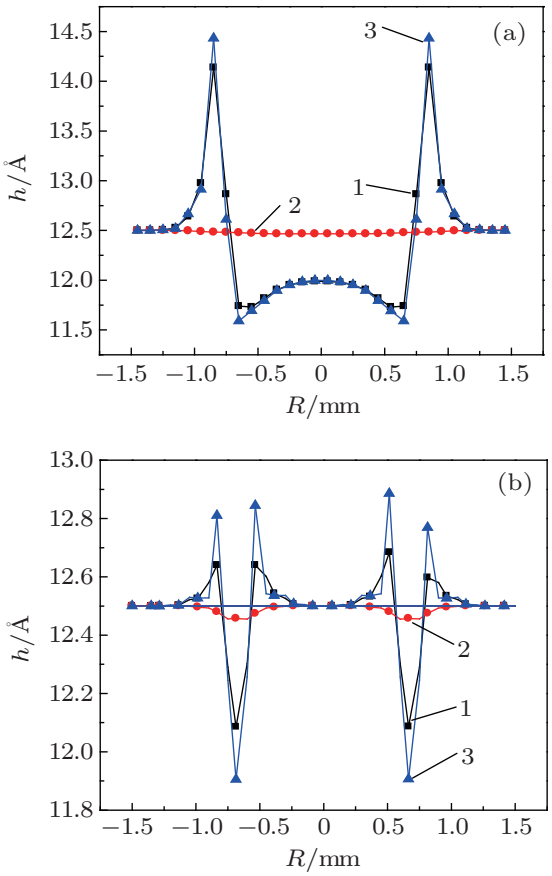


Fig. 12. (color online) Effects of Poiseuille flow and the Walcott flow on the film thickness deformation for (a) plane slider (1: all shearing stress, 2: no Poiseuille flow, 3: no Walcott flow).

As far as the van der Waals' force is concerned, when the lubricant film thickness is about 1nm, the film surface curvature changes as the air flows above the liquid with the lubricant film thickness of several nanometers. Therefore it is necessary to consider the effect of the surface tension. Figure 13 shows the influences of two kinds of body stress. It shows that the Laplace stress is not sensitive to the curve of lubricant thickness deformation. The Laplace stress can be ignored in the calculation because of the larger relative surface curvature and the smaller surface tension coefficient. The flow of the lubricant changes dramatically without the consideration of disjoining stress, indicating that the effect of disjoining stress on the flow of lubricant film must be considered.

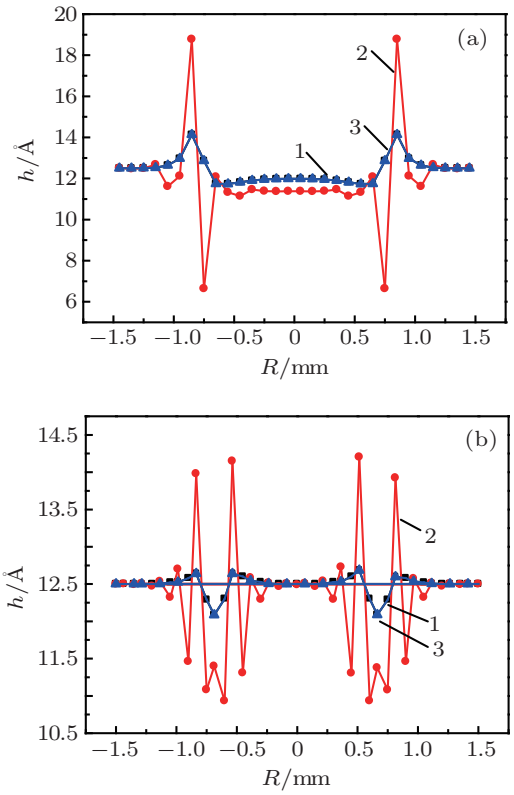


Fig. 13. (color online) Effects of disjoining stress and Laplace force stress on the film thickness deformation for (a) plane slider and (b) double-track slider (1: all force stress, 2: no disjoining stress, 3: no Laplace force).

3.3. Effects of working parameters on lubricant flow

The film thickness deformation changes with the variation of initial film thickness. Different initial thickness values (1.5 nm, 1.25 nm, 1 nm, and 0.75 nm) are used in simulation. The rotating speed is 5400 rpm, and flying height is 10 nm. As shown in Fig. 14, the absolute differences in actual maximum film thickness decrease remarkably with the decrease of the initial film thickness, and their deformations become consistent for both plane and double-track sliders, where $h_{\max}$ means the peak of lubricant and $h_{\min}$ refers to the bottom of the lubricant. The disjoining stress decreases down the fluctuation of lubricant film. It indicates that the decrease of thickness leads to the reduction of the lubricant flow at the same flying height.

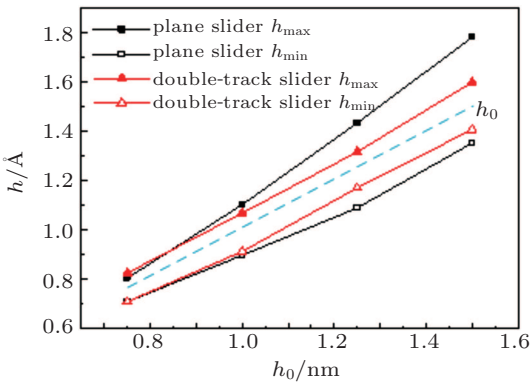


Fig. 14. (color online) The effect of initial film thickness on the film thickness fluctuation.

The change of flying height causes the transformation of the film thickness. When the initial film thickness is 1.25 nm with a rotating speed of 5400 rpm, for different flying heights, i.e., 10 nm, 8 nm, 5 nm, and 3 nm, the lubricant thickness values of the center section are shown in Fig. 15. As the flying height becomes smaller, the shape of lubricant film hardly changes. For the plane slider, lubricant thickness on both edges of the slider changes more prominently and the curvature close to the center of the slider grows larger with the decrease of flying height. For the double-track slider, the loss of lubricant is evident below the tracks and has little difference between two sides of the track.

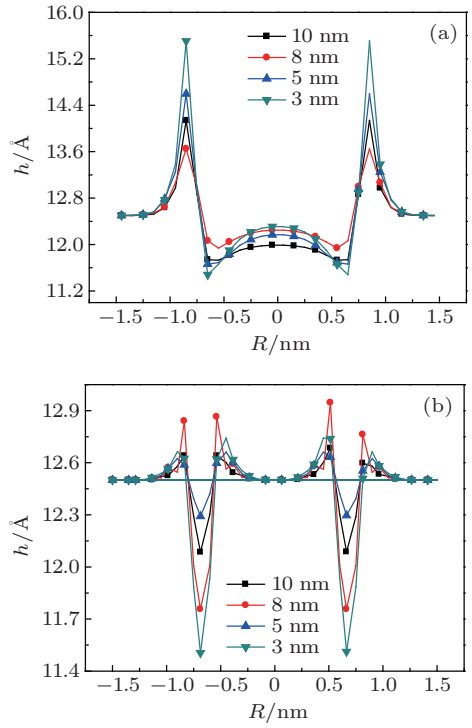


Fig. 15. (color online) Film thickness values at radial section for different flying heights of (a) plane slider and (b) double-track slider (initial film thickness is 1.25 nm).

The shearing force at the air bearing surface causes the lubricant flow. Figure 16 shows the shearing forces and the film thickness values for both plane and double-track sliders at different flying heights, in which F_τ is the shearing force (in unit N) and Δh is the distance between the peak and the bottom of the lubricant. The change of the shearing force is consistent with that of the film thickness deformation. The variation tendency is very apparent compared with the film thickness changes of plane slider.

The revolution speed determines the read/write efficiency, in other words, the faster the speed, the higher the efficiency is. The effect of revolution speed on film thickness is shown in Fig. 17. The initial film thickness is 1.25 nm, the flying height is 10 nm for different values of revolution speed n_w (in unit rpm). It can be seen from the results that the revolving speed has little effect on the shape of the lubricant thickness deformation.

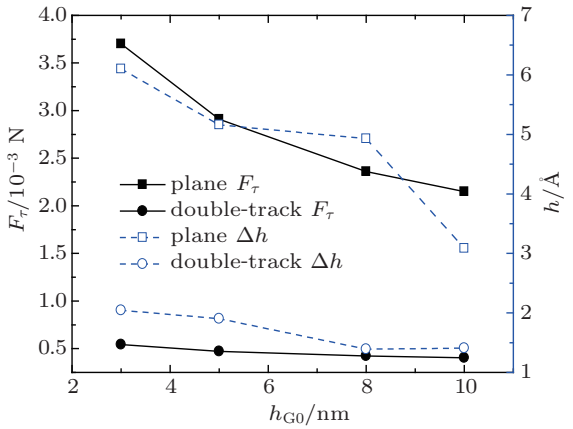


Fig. 16. (color online) Variations of shearing force and film thickness at different flying heights.

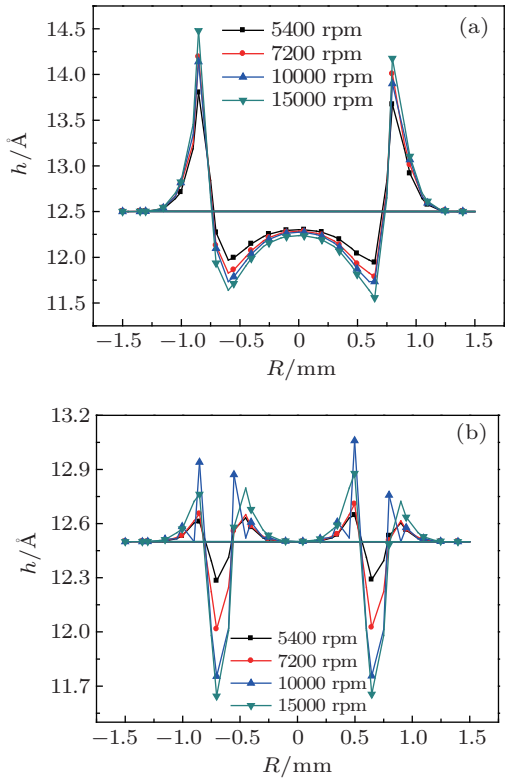


Fig. 17. (color online) Film thickness values at radial section for different revolving speeds at flying height 10 nm for (a) plane slider and (b) double-track slider.

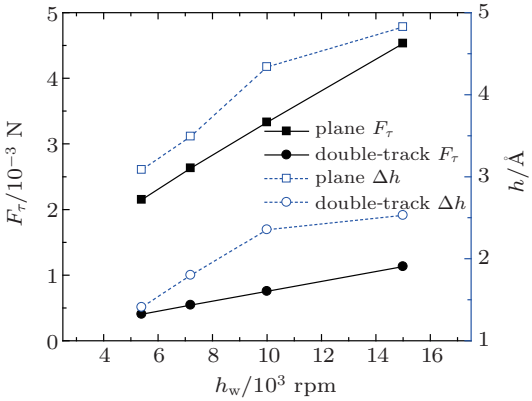


Fig. 18. (color online) Variations of shearing force and film thickness at different revolving speeds.

The shearing forces and the film thickness values at different revolution speeds are shown in Fig. 18. The film thickness deformation becomes much bigger with the speed and shearing force increasing, especially for the plane slider. The shearing forces increase linearly with the increase of revolving speed for different kinds of sliders.

4. Conclusions and perspectives

In the present study, the theoretical model of lubricant film thickness deformation at head/disk interface under the air dynamic pressure and the heat source is proposed, in which the effects of heat source and lubricant flow status (the Poiseuille flow and the Walcott flow) are considered. Two kinds of sliders with different structures are compared in the study of the air bearing stress distribution.

The effects of influencing factors such as air bearing stress with the consideration of rarefaction effect, van der Waals' force, surface tension and external stress on the flow and depletion characteristics of lubricant film are discussed. It is found that the shearing stress is the decisive factor which leads to the change of lubricant film thickness, and the disjoining stress leads to the recovery of the lubricant. The Poiseuille flow is the main factor which leads to the shearing stress. Under the heat source condition, the laser causes the lubricant viscosity and the lubricant evaporation to decrease. The higher the power of the laser, the faster the evaporation of the lubricant film is.

As far as the working parameters are concerned, it is found that from the comparison of simulation results the lubricant film thickness has little fluctuation on a small initial lubricant film thickness. The increase of revolving speed causes the higher air bearing pressure, leading to a higher fluctuation in lubricant film thickness. These effects are related to the slider structure. In the present case, when the flying height is 10 nm and the revolution speed is 5400 rpm, the lubricant film thickness deformation will not change sharply.

References

[1] Wu A Q, Kubota Y, Klemmer T, *et al*. 2013 *IEEE Trans. Magn.* **49** 779
[2] Ji R, Dao T K L, Xu B X, *et al*. 2011 *IEEE Trans. Magn.* **47** 1988
[3] Watanabe T and Bogy D B 2002 *IEEE Trans. Magn.* **38** 2138
[4] Li X, Hu Y Z and Wang H 2005 *Acta Phys. Sin.* **54** 3787 (in Chinese)
[5] Guo Q, Izumisawa S, Phillips D M, *et al*. 2003 *J. Appl. Phys.* **93** 8707
[6] Jing H D, Zhang X J, Tian Y M, *et al*. 2015 *Acta Phys. Sin.* **64** 168101 (in Chinese)
[7] Ma Y, Liu B 2007 *Appl. Phys. Lett.* **90** 143516
[8] Shi B J, Ji J Dand Yang T Y 2011 *Microsystem Technol.* **17** 1271
[9] Matsuoka H, Oka K, Yamashita Y, *et al*. 2011 *Microsystem Technol.* **17** 983
[10] Kasai P H and Raman V 2012 *Tribology Letters* **48** 367
[11] Bhushan B and Tonder K 1989 *J. Tribology* **111** 228
[12] Fukui S and Kaneko R 1988 *J. Tribology* **110** 253
[13] Marchon B, Karis T, Dai Q, *et al*. 2003 *IEEE Trans. Magn.* **39** 2447